Flexural fatigue and fracture toughness behavior of nanoclay reinforced carbon fiber epoxy composites

Md Sarower Hossain Tareq[1] ⓘ, Shaik Zainuddin[2] ⓘ,
Mahesh V Hosur[3], Bodiuzzaman Jony[4] ⓘ,
Mohammad Al Ahsan[2] and Shaik Jeelani[2]

Abstract

3-point flexural fatigue and Mode I interlaminar fracture tests were done to study the fatigue life and fracture toughness of nanoclay added carbon fiber epoxy composites. Fatigue life data was analyzed using Weibull distribution function, validated with Kolmogorov-Smirnov goodness-of-fit, and predicted by combined Weibull and Sigmoidal models, respectively. The nanophased samples showed more than 300% improvement in mean and predicted fatigue life. At 0.7 stress level, the nanophased samples passed the 'run-out' fatigue criteria (10^6 cycles), whereas, the neat samples failed much earlier. The interlaminar fracture toughness of nanophased samples was also enhanced significantly by 71% over neat samples. Optical and scanning electron microscopic images of the nanophased fractured samples revealed certain features that improved the respective fatigue and fracture properties of the composites.

Introduction

Carbon fiber reinforced polymer (CFRPCs) composites are extensively used in load bearing applications as light weight structural components in aircraft, automotive and wind turbine industries, among others.[1,2] Most of these applications are associated with cyclic loading that makes fracture due to fatigue one of the most important failure modes in the CFRPCs.[3–5] Fatigue failure occurs in composites by gradual degradation of stiffness due to initiation and propagation of various damage modes upon continuous application of cyclic loads.[6–8] In transverse loading condition, interlaminar characteristics directly control the fatigue performance of the laminated composites. Therefore, studies of fatigue behavior in combination with fracture toughness and delamination resistance are important to accurately understand the transverse fatigue behavior of the CFRPCs.

Researchers have noted that CFRPCs showed excellent fatigue performance in tensile loading which is mostly dominated by fibers.[9–12] However, under transverse loading, failure behavior is governed by matrix and fiber-matrix interfacial bonding properties, which are generally lower than that of fibers and hence CFRPCs are more vulnerable to fail at lower loads in transverse direction than when applied along the fiber directions.[13–15] Under transverse loadings, cracks initiate in the matrix phase in between the fibers that by propagating causes matrix cracking and fiber-matrix debonding resulting in overall degradation of stiffness. Fiber-matrix bonding failure occurs both within a ply as well as between the plies. Therefore, researchers have

[1]Department of Materials Engineering, Purdue University, USA
[2]Department of Materials Science and Engineering, Tuskegee University, USA
[3]Frank H. Dotterweich College of Engineering, Texas A&M University-Kingsville, USA
[4]Department of Aerospace Engineering and Mechanics, University of Alabama, USA

Corresponding author:
Shaik Zainuddin, Tuskegee University, 100 Chappie James Center, Tuskegee, AL 36088, USA.
Email: szainuddin@tuskegee.edu

been investigating various means to obtain improved transverse properties of the CFRPCs by enhancing the fracture toughness of the matrix and achieving strong fiber-matrix bonding.

Among several approaches to achieve this objective, addition of nanoparticles in the epoxy matrix has been considered to be the most promising to improve transverse mechanical properties in the FRPCs.[8,16] Green et al. added carbon nanofibers (CNFs) in epoxy matrix and observed 20% and 26% increased flexural strength and modulus of CFRPCs, respectively.[17] Addition of AlO_2 and TiO_2 nanoparticles significantly improved fatigue crack resistance of the epoxy matrix.[18] 60 to 250% improved tensile fatigue life was achieved by Grimmer et al. when they added 1% CNTs in epoxy matrix.[19] Among the potential nanofillers, nanoclay was most widely studied because of its low cost and ease of dispersion along with promising improvement in matrix dominated properties.[20–23] Researchers have reported significant improvement in impact properties, fracture toughness and mode I delamination resistance of FRPCs by incorporating nanoclay in the epoxy matrix.[22,24–26] Kumar et al. reported 113.7% improvement in flexural strength[21] and Zabihi et al. showed 32% improved shear strength by adding nanoclay in CFRPCs.[27] Khan et al. reported 74% increased tensile fatigue life of CFRPCs after incorporating nanoclay.[11]

Although there have been several efforts to improve the static properties of CFRPCs by means of addition of nanoclay, reported works in open literature on fatigue performance of CFRPCs containing nanoclay are very scarce. In addition, most of the works found on fatigue performance of nanoparticles added CFRPCs are focusing on tensile fatigue rather than flexural fatigue.[11,28] Improvement of flexural fatigue is more challenging being mostly dominated by matrix and interfacial properties of the composites. In that regards, there is an emerging demand to investigate the effect of nanoclay, promising nanofiller to improve matrix performance, on the flexural fatigue performance of CFRPCs.

Fatigue life data obtained are usually scattered because of the anisotropic and heterogenetic structure of the FRPCs, and therefore, conventional S-N curve is not appropriate to accurately describe and predict fatigue life of FRPCs.[29–32] Among various statistical methods such as the exponent distribution, normal distribution, lognormal distribution and Crow-AMSAA analysis, two parameter Weibull distribution function has been most widely used for failure analysis of materials.[30,33,34] Weibull distribution is a established model for fatigue life analysis of laminated composites because it can reasonably model wide range of distributed data, provide more information about fatigue life including failure probability and failure mode.[35–37] In addition, stiffness degradation with fatigue cycles is an important measurement to clearly present fatigue performance and life prediction for the laminated composites.[29,33,38,39]

The aim of this work, therefore, is to systematically investigate the fatigue performance and fracture toughness of the CFRPCs reinforced with nanoclay and compare it with control CFRPCs. In this regard, 3-point flexure fatigue test and mode I interlaminar fracture test have been carried out. Fatigue life was analyzed and predicted as a function of failure probability using Weibull distribution function and Sigmoidal model. The Weibull parameter was validated using Kolmogorov-Smirnov goodness-of-fit test. Kolmogorov-Smirnov test is non-parametric and does not depend on the cumulative distribution function, thus more reliable to test data validity.[40] Stiffness degradation and residual fatigue properties were also presented to describe and compare the fatigue performance of the CFRPCs. Fracture toughness result was calculated following four different data reduction techniques, i.e., visual inspection (VIS) from the recorded video, non-linearity (NL), 5% increase in compliance (5% COM↑) and peak load (PEAK). Finally, the microstructure of the fractured flexure specimens after static and fatigue loading were investigated by SEM and described correlating the respective fatigue and fracture toughness result.

Materials and fabrication

Materials

Eight harness satin weave carbon fabrics with 3k tow size and thickness of 0.46 mm was purchased from US Composites Inc. SC-15 epoxy resin was obtained from Applied Poleramic, Inc., California, USA. Montmorillonite nanoclay (Nanomer® I. 30 E), MMT used was supplied by Sigma-Aldrich Co., USA. The nanoclay was surface modified by 25–30 wt.% octadecylamine.

Dispersion of nanoclay and fabrication of CFRPCs

Nanoclay reinforced CFRPCs were fabricated using 2 wt. % loading of MMT, since most of the previous works have shown the optimum mechanical properties of the MMT reinforced CFRPCs were obtained for 2 wt.% loading.[25,26] At first, 2 wt. % nanoclay was dried at 100°C for 2 hours to remove moisture and avoid lump formation. The dried nanoclay was then mixed with part A of SC-15 epoxy resin manually, followed by magnetic stirrer at 800 rpm for 3 hours at 40°C. The unmodified (neat) and modified

(nanoclay added) resin part A was then mixed with the resin part B (hardener) at a ratio of 10:3, respectively.

CFRPCs were fabricated using the neat and nanoclay added epoxy resin followed by hand layup and compression mold processes. The resin was at first interspersed between ten layers of woven carbon fabric using a hand roller and laid between porous Teflon, bleeder cloth and non-porous Teflon. To make samples with pre-crack for fracture toughness test, a 12.5 μm thick and 38 mm wide Teflon film was inserted at the mid-plane of one end of the laminate during the layup process.

The setup was then placed in compression mold and cured for 4 hours at 60°C while maintaining 1-ton pressure. The composites were finally post-cured at 100°C for 2 hours and the temperature was gradually reduced to avoid any thermal residual stresses. The thickness of the laminate obtained was between 3.5 to 3.65 mm.

Experimental

Static test

Three-point static flexure test was performed using MTS 810 (MTS System Corp., USA) machine (using 5 KN load cell) according to the ASTM D790-03. The test was conducted at a crosshead speed of 1.2 mm/min, while maintaining sample thickness to span ratio of 1:16. At least five specimens of each set were tested to find the average flexural strength and modulus. As the deflection of the specimens at maximum force did not exceed over 5% of support span, according to ASTM D790-03, the flexural stress and modulus were calculated using equation (1) and (2), respectively.

$$\sigma_f = \frac{3FL}{2bd^2} \tag{1}$$

$$E_f = \frac{L^3}{4bd^3} m \tag{2}$$

Where F, σ_f, and E_f corresponds to the maximum load, maximum flexural strength, and modulus, respectively; b, d and L are the width, thickness and length of support span (mm), respectively; m in equation (2) is the initial slope of load-deflection curve (N/mm). 3-point flexural test setup is shown in Figure 1(a).

Fatigue test

Three-point flexural fatigue test was performed in the same machine (MTS 810 and 5 KN load cell) according to the specifications of ASTM D7774-17.[41] The test was conducted in constant amplitude sinusoidal load control mode at a stress ratio of 0.1 and frequency of 5 Hz. Samples were tested at four different stress levels, S = 0.9, 0.8, 0.75 and 0.7 respectively, where S is the ratio of applied stress to the ultimate flexural stress obtained from the static test. At least 5 specimens were tested for each stress level up to 1 million (1×10^6) cycles that is generally defined as "run-out" fatigue criteria. The test termination criteria was defined as the 25% drop of the responded load or the tests were manually stopped when the samples met the "run-out" criteria of 10^6 cycles. To examine the degradation in properties due to fatigue loading, the tests were terminated after a certain number of cycles as listed in the Table 1 and a static flexural test was performed. At least three specimens have been tested for each condition.

Mode I interlaminar fracture toughness test

To evaluate the Mode I interlaminar fracture toughness (G_I), interlaminar fracture test was performed in the double cantilever beam (DCB) configuration according to the ASTM D5525-13.[42] The test was conducted in the displacement control mode (0.06 mm/sec) in MTS Qtest-25 universal test frame with 2 KN load cell at room temperature (23°C). DCB specimen of dimensions $216 \times 38 \times 3.65$ mm with a 38 mm pre-crack created through a Teflon insert was used to perform the test. The critical fracture toughness G_{Ic} was calculated according to the modified beam theory (MBT) that includes both shear deformation and crack-front rotation in the calculation. According to the MBT, G_{Ic} is:

$$G_{IC} = \frac{3P\delta}{2b(a + |\Delta|)} \tag{3}$$

Where, P, δ, a and b represent the load, crosshead displacement, crack length and specimen width respectively. Δ is the crack length correction term which was calculated by plotting cube root of the compliance ($C^{1/3}$) with respect to the crack length (a). Canon 57x high-resolution video recorder was used to track the crack propagation and the load displacement data was recorded at regular intervals. The DCB test setup is shown in Figure 1(b).

Result and discussion

Static flexural behavior

Figure 2 represents a representative stress-strain plot for the control and nanoclay added CFRPCs, and the flexural strength and modulus values are given in Table 2. From Table 2, it is seen that nanoclay added
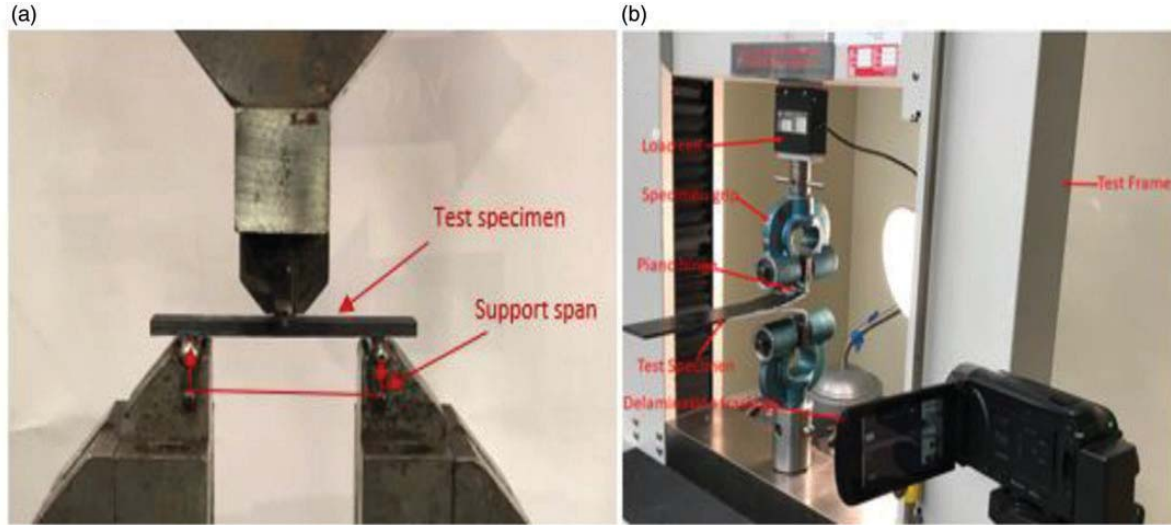
Figure 1. (a) 3-point flexural static and fatigue test setup, (b) DCB test setup during delamination growth in Mode I interlaminar fracture test.

Table 1. Static test performed after number of fatigue cycles to investigate the residual fatigue properties.

Types	S = 0.8	S = 0.7
Control CFRPCs	5000	50000
Nanoclay CFRPCs	5000	50000

samples showed 14.7% improvement in flexural strength and 23.8% improvement in flexural modulus compared to the control samples. Figure 2 also shows that nanoclay added CFRPCs can withstand higher load beyond the yield point with higher strain to failure than the control CFRPCs, which is also consistent with the previous observations.[43]

Optical microscopy images of the fracture specimens after static test are shown in Figure 3. It is seen that fracture region of the control specimen is associated with several delamination and matrix cracking along with fiber breakage. Whereas, nanoclay added specimen showed no considerable delamination and matrix cracking compared to the control specimen and fiber breakage is the major failure mode in these specimens. Under static flexural loading, laminated composites experience compressive and tensile stress at the upper and lower side of the specimen, respectively. From Figure 3, it is seen that control CFRPC shows significant fracture area at compressive side of the specimen because of delamination and matrix cracking. Whereas, nanoclay added CFRPC showed no considerable delamination type of fracture in the compressive side. Rather, nanoclay added CFPRCs mainly fractured at the tensile region by means of fiber breakage. This is an indication of the improved fiber-matrix interfacial

bonding and stronger matrix of the nanoclay added samples that reduced the cracking and delamination. Consequently, nanoclay added CFRPCs mainly failed by means of fiber breakage and showed better performance under compressive loading. Strong interfacial bonding of the nanoclay specimen is clearer from the SEM images of the fracture fiber bundle, as seen in Figure 4. Fibers of control specimen are showing debonding and brush-like separation with smooth surface, whereas, nanoclay specimen is associated with strong bonded fibers and rough surface even after fracture. Because of the high aspect ratio and active functional group at the surface, nanoclay effectively increased matrix-fiber interaction and improved the interfacial bonding.[44]

Fatigue life assessment

Fatigue test result. Figure 5 provides the information on the tested fatigue life with respect to the four stress levels for control and nanoclay added CFRPCs. It is seen that at all stress levels, nanoclay added samples exhibited significantly longer fatigue life than their control counterparts. At stress levels of 0.9, 0.8 and 0.75, mean fatigue life of the nanoclay added CFRPCs was found to be higher than the control CFRPCs by 687%, 327% and 384%, respectively (Table 3). At 0.7 stress level, all of the nanoclay added samples demonstrated infinite fatigue life as they exceeded "run-out" fatigue criteria (10^6 cycles), whereas, majority (80% among tested) of the control samples when tested at 0.7 stress level failed at less number of fatigue cycles than the "run-out" criteria. Fatigue data for nanoclay added samples at stress level 0.7 are seen to be clustered in a small region, since the tests were manually stopped
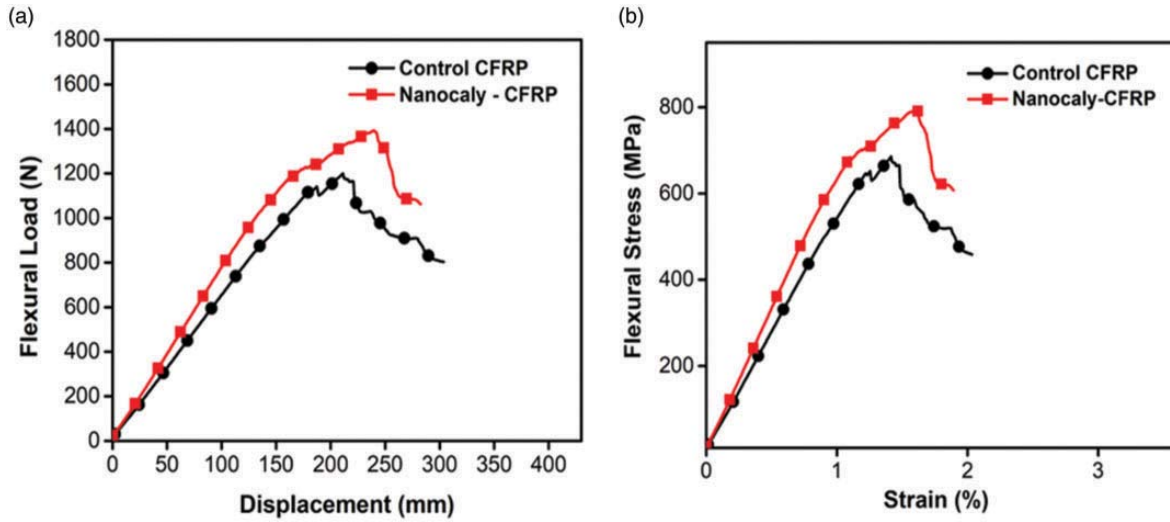
Figure 2. (a) Load-displacement plot and (b) Stress-strain plot of the control and nanoclay added CFRPCs in the 3-point static flexure test.

Table 2. Static flexural properties for control and nanoclay added CFRPCs.

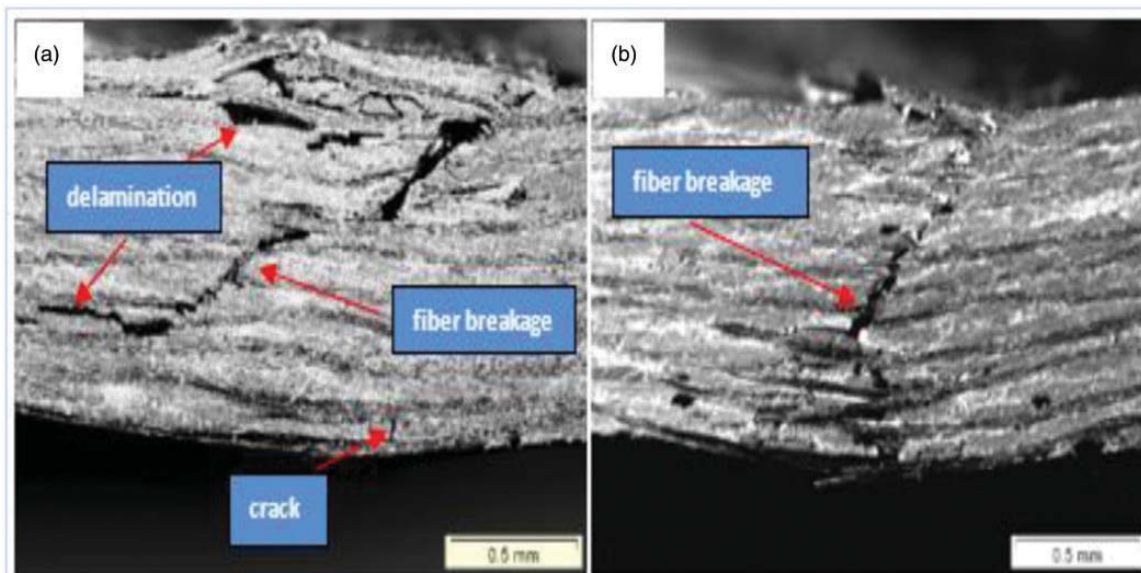| Sample types	Flexural strength (MPa)	% Change	Flexural modulus (GPa)	% Change
Control CFRPCs	680 ± 11.5	–	55.6 ± 1.3	–
Nanoclay – CFRPCs	780 ± 24.1	+14.7	68.9 ± 3.5	+23.8

Figure 3. Optical microscopic image of fracture specimen after static flexure test. (a) control CFRPC, (b) nanoclay–CFRPC.

when the number of fatigue cycles for these specimens were found to exceed the "run-out" criteria. Fatigue life of the composites are dependent on the stress ratio, R at a given frequency.[45,46] Higher stress ratio results in lower alternating stress during fatigue test, and composite specimen experience fluctuation over lower amplitude range. Therefore, both types of the CFRPCs are expected to show comparatively higher
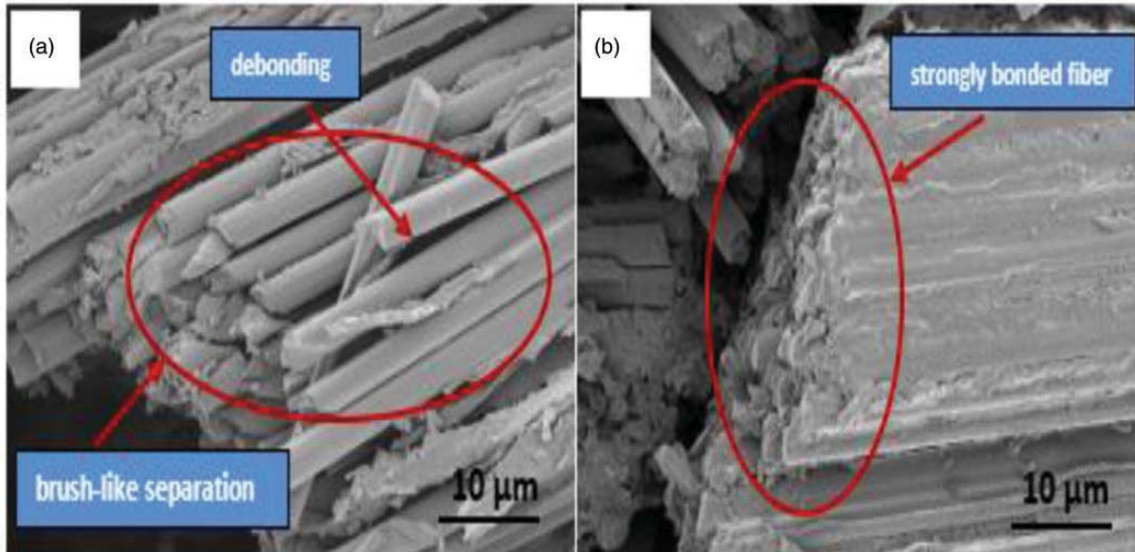
Figure 4. Fiber bundle of fractured specimen after static flexure test. (a) control CFRPC and (b) nanoclay – CFRPC.
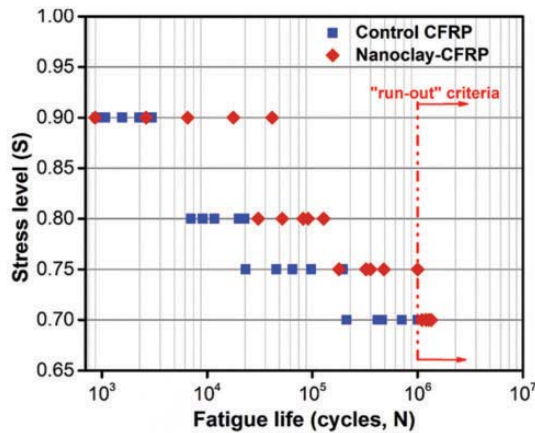

Figure 5. Tested fatigue life in respect to the four stress levels for the control and nonoclay added CFRPCs.

Table 3. Comparison of mean fatigue life of the control and nanoclay added CFRPCs.

Types	Mean fatigue life			
Stress level	0.9	0.8	0.75	0.7
Control CFRPCs	1759	17926	85278	558561
Nanoclay – CFRPCs	13844	76523	412571	>1000000
Improvement	687%	327%	384%	infinite life achieved

fatigue life, respectively, with increasing value of stress ratio, R.[47]

Fatigue failure in the laminated composites occurs by the formation of cracks that grow and coalesce faster under the fluctuating load compared to the static load.[11] Presence of nanoclay in the epoxy matrix reduces polymer chain mobility and increases the stiffness of the matrix. Stiffer matrix along with the strong interfacial bonding facilitates improved overall stress transfer of the composite under fluctuating load. In addition, presence of nanoclay in epoxy matrix in between the fibers suppresses and delays the initiation, growth and coalescence of the cracks. Consequently, it requires higher loads and more number of cycles for the damage initiation and growth in case of samples where nanoclay was used to improve the properties of matrix, fiber-matrix interface and thereby those of the FRPs themselves.

However, it is to be noted that the distribution of fatigue life data is considerably scattered because of heterogeneous nature of FRP composites. Therefore, conventional stress vs. fatigue life plots are not appropriate to accurately describe fatigue behavior of FRP composites. In addition, it is reasonable to describe fatigue life with reliable statistical function including failure probability, and to consider some other related aspects such as stiffness degradation with fatigue cycles and residual fatigue properties.

Weibull distribution analysis. The two-parameter Weibull distribution analysis was performed to characterize and compare the flexural fatigue performance of the CFRPCs without and with nanoclay. The cumulative

Table 4. Fatigue life data calculation for the Weibull distribution analysis at stress level of 0.8.

Types	i	N	L_R	$\ln(\ln(1/L_R))$	$\ln(N)$
Control CFRPCs	1	7019	0.8571	−1.8698	8.8564
	2	9096	0.7143	−1.0892	9.1156
	3	11730	0.5714	−0.5805	9.3699
	4	20065	0.4286	−0.1657	9.9067
	5	22738	0.2857	0.2254	10.0318
	6	36908	0.1429	0.6657	10.5162
Nanoclay − CFRPCs	1	30559	0.8333	−1.7020	10.3274
	2	51660	0.6667	−0.9027	10.8524
	3	81748	0.5000	−0.3665	11.3114
	4	90954	0.3333	0.0940	11.4181
	5	127696	0.1667	0.5832	11.7574

distribution function, $F(N)$ of the Weibull analysis is expressed as follows:[48]

$$F(N) = 1 - \exp\left(-\left(\frac{N}{\beta}\right)^{\alpha}\right) \qquad (4)$$

Where α is the shape parameter (Weibull slope) and β is the scale parameter (characteristic life) at a specific stress level, S. The graphical method was followed to determine both α and β by plotting the Weibull distribution data. The survivorship function or reliability function, L_R for Weibull analysis is defined as,

$$L_R = 1 - F(N) \qquad (5)$$

After substituting the value of $F(N)$ from equation (5) and taking logarithm on both side, equation (4) can be expressed as:

$$\ln\left(\ln\frac{1}{L_R}\right) = \alpha\ln(N) - \alpha\ln(\beta) \qquad (6)$$

Equation 6 represents linear relationship. To plot this equation, the fatigue lives data for a specific stress level S have been arranged in ascending order. The empirical survivorship function L_R for each fatigue life data at a specific stress level were obtained from the following relationship:[49]

$$L_R = 1 - \frac{i}{k+1} \qquad (7)$$

Where i denotes the specimen order number and k stands for the total number of the specimens tested at a particular stress level.

Table 4 presents the typical fatigue life data calculation at stress level of 0.8 to determine the parameter α and β by means of graphical method. Stress level of 0.8 was chosen as a representative to describe the behavior of the samples tested in the current study. At other stress levels, the behavior is similar and showing at other stress levels does not make significant intellectual value to the discussion. As shown in Figure 6, from equation (6) the expression $\ln(\ln(1/L_R))$ has been plotted against $\ln(N)$ at each stress level for both control and nanoclay added CFRPCs, respectively. The data was fitted using linear regression analysis to determine the shape parameter α and the scale parameter β as listed in Table 5 for both types of the CFRPCs. The shape parameter α was determined from the slope of the line and the characteristic life β correspond to the fatigue life at $F(N) = 0.632$. As seen from the Figure 6, a good correlation coefficient $R^2 > 0.93$ was achieved for each stress level indicates strong statistical confidence, and that the Weibull distribution model can reasonably characterize the fatigue life of the CFRPCs, both without and with nanoclay.

Goodness-of-fit test. To further validate the value of α and β obtained from Weibull analysis, Kolmogorov-Smirnov goodness-of-fit test was performed at a 5% significant level using the following equation[40]:

$$D_1 = \max\left|\frac{i}{k} - F(N_i)\right| \qquad (8)$$

Where $F(N_i)$ denotes the theoretical cumulative distribution obtained from the equation (4) for the fatigue life N_i of ith specimen arranged in the ascending order at any specific stress level. In order for the model to be accepted by the Kolmogorov-Smirnov test, the condition $D_1 < D_c$ should be satisfied. The value of D_c is obtained from the Kolmogorov-Smirnov table[50] based on the number of specimens tested and the level of significance. Table 6 shows the typical calculation to determine the Kolmogorov-Smirnov parameter
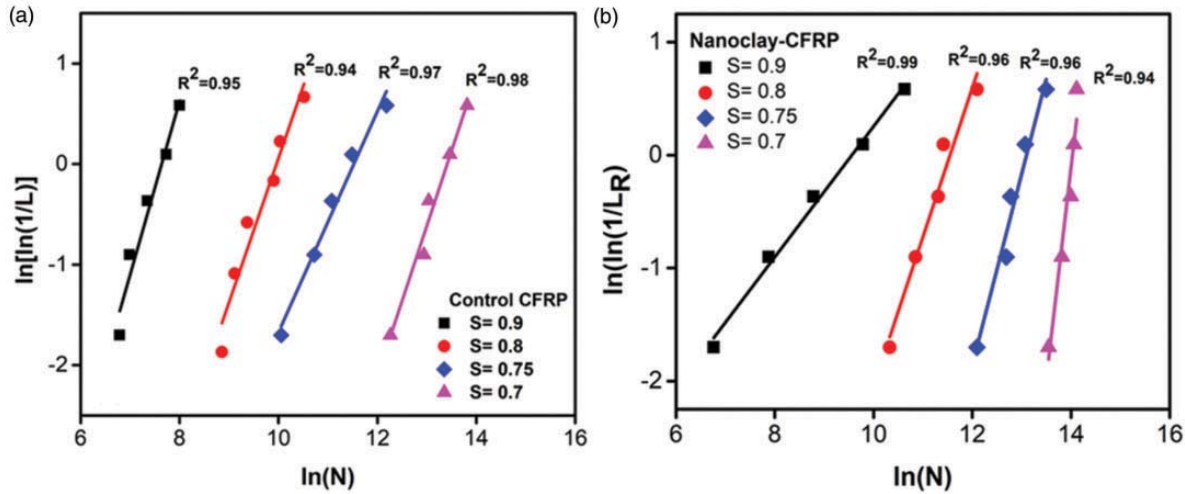
Figure 6. Flexural fatigue life distribution of (a) control and (b) nanoclay added CFRPCs under different stress level, S according to the Weibull model.

Table 5. The Weibull distribution parameters at various stress level, S for the control and nanoclay added CFRPCs.

Stress level, S	Control CFRPCs		Nanoclay − CFRPCs	
	Shape parameter, α	Scale parameter, β	Shape parameter, α	Scale parameter, β
0.9	1.726	2072	0.578	14268
0.8	1.433	21123	1.319	104057
0.75	1.098	101543	1.691	489492
0.7	1.492	664976	3.734	1240551

Table 6. Calculation of Kolmogorov-Smirnov test parameter D_1 for stress level S = 0.8.

Types	i	N	i/k	$F(N_i)$	D_1
Control CFRPCs	1	7019	0.1667	0.1863	0.0197
	2	9096	0.3333	0.2584	0.0749
	3	11730	0.5000	0.3498	0.1502
	4	20065	0.6667	0.6051	0.0616
	5	22738	0.8333	0.6709	0.1624
	6	36908	1.0000	0.8919	0.1081
Nanoclay − CFRPCs	1	30559	0.2000	0.1802	0.0198
	2	51660	0.4000	0.3277	0.0723
	3	81748	0.6000	0.5168	0.0832
	4	90954	0.8000	0.5671	0.2329
	5	127696	1.0000	0.7302	0.2698

D_1 at stress level of 0.8. The greatest value of D_1 obtained from any specific stress level was compared to the respective D_c value. As shown in Table 7, for all sets of specimens, the calculated value of D_1 is much smaller than the respective D_c value for both types of the CFRPCs. Therefore, it can be concluded that two-parameter Weibull distribution analysis is suitable to

predict the flexural fatigue life of control and nanoclay added CFRPCs.

Failure probability and prediction of fatigue life. Prediction of flexural fatigue lives have been performed as a function of the failure probability, P_f and the number of fatigue cycles, N at each stress level. Substituting $P_f = F(N)$ in

Table 7. Kolmogorov-Smirnov goodness-of-fit test results for the Weibull analysis of the flexure fatigue life distribution of control and nanoclay added CFRPCs.

Types	Stress level, S	Goodness-of-fit parameter, D_I	Critical value, D_c	$D_I < D_c$
Control CFRPCs	0.9	0.1521	0.5633	Accepted
	0.8	0.1624	0.5193	Accepted
	0.75	0.1835	0.5633	Accepted
	0.7	0.1618	0.5633	Accepted
Nanoclay – CFRPCs	0.9	0.1569	0.5633	Accepted
	0.8	0.2698	0.5633	Accepted
	0.75	0.1835	0.5633	Accepted
	0.7	0.7000	0.5633	Accepted

equation (4), the equation for the failure probability is obtained as follows:

$$P_f = 1 - \exp\left(-\left(\frac{N}{\beta}\right)^{\alpha}\right) \quad (9)$$

Where α and β are the shape and scale parameter respectively at a specific stress level obtained from the Weibull analysis and N is the fatigue life of any specimen under the respective stress level. The Sigmoidal model was used to correlate the calculated P_f and the logarithm of fatigue life, $\log(N)$:[51]

$$P_f = \frac{A_1 - A_2}{1 + \exp(\log N - \log N_0)/\Delta N} + A_2 \quad (10)$$

Where A_1, A_2, N_0 and ΔN are the constant. The plots showing the predicted fatigue life for both types of the CFRPCs have been presented in Figure 7(a) to (c) at the stress levels of S = 0.9, 0.8 and 0.75, respectively. The correlation coefficient R^2 for all the plots was found to be >0.96. Since the value of R^2 is very close to 1, it implies that the Sigmoidal model can well represent the fatigue failure probability of the CFRPCs both without and with nanoclay.[52]

A common feature of the three plots is that, at a specific stress level the failure probability increases with increasing fatigue cycles. It is also clear that for a certain value of failure probability P_f, nanoclay added samples have shown significantly higher fatigue life than the control samples, given a particular stress level. Table 8 lists the comparison of the predicted fatigue life of both types of the CFRPCs for 50% failure probability (median lives, $P_f = 0.5$) and 63.5% failure probability (characteristic lives, $P_f = 0.639$. It is seen that at 50% failure probability, nanoclay added CFRPCs resulted in 352%, 382% and 442% longer fatigue life at stress levels of 0.9, 0.8 and 0.75 respectively compared to the control CFRPCs.

Failure probability for S = 0.7 was not listed or plotted for the comparison, since testing for the nanoclay added samples at 0.7 stress level was manually stopped due to fatigue cycles exceeding the "run-out" criteria. At 0.7 stress level nanoclay added CFRPCs are regarded to withstand infinite fatigue life.

Stiffness degradation. Stiffness degradation with fatigue cycles of the control and nanoclay added CFRPCs have been presented and compared in Figure 8. The stiffness degradation has been presented as a function of normalized stiffness vs. fatigue cycles at each stress level (Figure 8(a) to (d)), respectively. Normalized stiffness is defined as the ratio of the stiffness of nth fatigue cycle (E_n) to the stiffness of 1st fatigue cycle (E_1) at the respective stress level. From the Figures, it is seen that regardless of the stress level, nanoclay added CFRPCs exhibited higher residual normalized stiffness throughout the whole fatigue life. Table 9 shows the number of cycles required for 10% reduction in the stiffness for both control and nanoclay added CFRPCs. From Table 9, it is seen that nanoclay added samples have demonstrated significantly higher number of fatigue cycles than the control samples before undergoing 10% reduction in stiffness. For example, at 0.9 stress level the number of cycles required is 20 times higher for nanoclay added samples than the control samples.

At 0.7 stress level, nanoclay added samples showed no considerable degradation in stiffness until the "run-out" criteria (Figure 8(d)), after which the test was manually terminated. In contrast, control samples at 0.7 stress level, showed sudden stiffness degradation at about 10^5 fatigue cycles that ultimately led the samples to fail (Figure 8(d)). It is also seen from Figure 6 that for control CFRPCs the degradation at higher stress levels (S = 0.9, 0.8) is faster than at a lower stress level, whereas, for nanoclay added CFRPCs degradation rate did not show much dependency on the stress level.
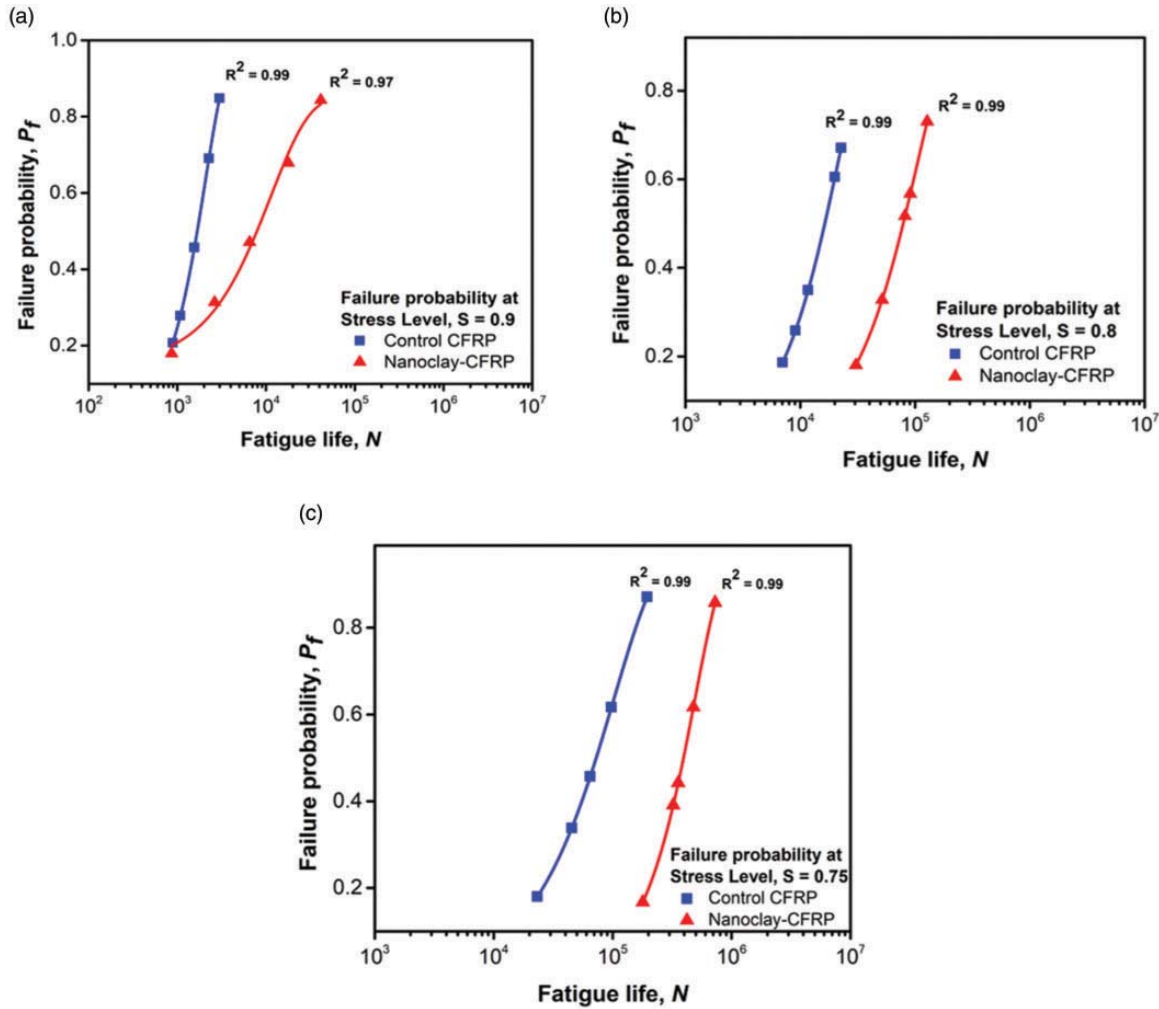
Figure 7. Comparison of the predicted fatigue life of control and nanoclay added CFRPCs at three stress levels (a) S = 0.9, (b) S = 0.8, (c) S = 0.75. The curves were fitted using the Sigmoidal model.

Table 8. Predicted fatigue life at failure probability of $P_f = 0.5$ (median lives) and $P_f = 0.632$ (characteristic lives) for control and nanoclay added CFRPCs.

	Predicted fatigue life at $P_f = 0.5$			Predicted fatigue life at $P_f = 0.632$		
Types	0.9	0.8	0.75	0.9	0.8	0.75
Control CFRPCs	1675	16356	72724	1319	12265	49949
Nanoclay − CFRPCs	7568	78812	394108	3707	57647	308801
Improvement	352%	382%	442%	181%	370%	518%

Meanwhile, all of the figures show almost similar trend of stiffness degradation with increasing number of fatigue cycles. The stiffness degradation trend for both types of the samples is characterized by the slow degradation of initial stiffness followed by the faster degradation rate prior to the ultimate failure.

Residual fatigue properties. To investigate the residual properties, static flexure test was performed by terminating the fatigue test after a certain number of cycles as listed in Table 1. Residual static tests were performed after 5k cycles for samples tested at a stress level of 0.8 and after 50k cycles for samples tested at
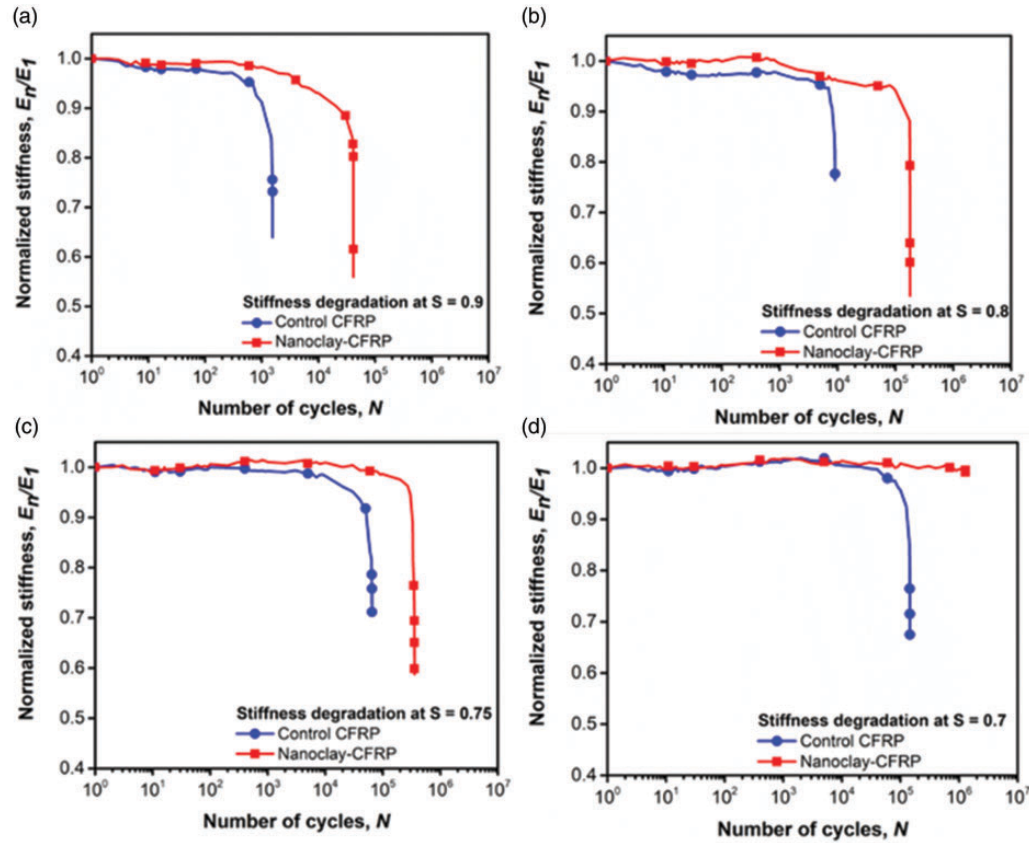
Figure 8. The variation of the normalized stiffness with the number of fatigue cycles of control and nanoclay added CFRPCs at different stress level, (a) S = 0.9, (b) S = 0.8, (c) S = 0.75, (d) S = 0.7.

Table 9. Comparison of the fatigue cycles required for 10% reduction in the stiffness for control and nanoclay added CFRPCs.

	Number of cycles required for 10% reduction in stiffness			
Types	S = 0.9	S = 0.8	S = 0.75	S = 0.7
Control CFRPs	1000	8000	55000	130000
Nanoclay – CFRPs	20000	150000	310000	infinite

a stress level of 0.7, results of which are illustrated in Figure 9. From Figure 9(a), it is seen that loss of flexural strength after specific number of fatigue cycles was more than twice (in terms of percentage) for the control samples than the corresponding nanoclay added samples. For example, after 5k cycles at 0.8 stress level, control samples lost about 18% of its initial flexural static strength, whereas the loss was only 7% in case of nanoclay added samples. Loss of flexural modulus for control samples after 5k (at S = 0.8) and 50k (at S = 0.7) fatigue cycles was about 5 times and 3 times higher than the corresponding nanoclay added samples. The stiffness degradation plot in Figure 8 also supports this. Another important observation that can be seen from Figure 9 is that even after 50 K cycles at stress level of 0.7, the residual strength and stiffness of nanoclay sample is much higher than the static strength and stiffness of neat sample. From Figures 8 and 9, it is reasonable to mention that nanoclay added CFRPCs hold higher residual strength and stiffness than the control CFRPCs throughout the fatigue life. Incorporation of nanoclay in the epoxy matrix significantly improved the bonding strength in the fiber-matrix interfacial region. Improved bonding and tortuous nature of nanoclay in the epoxy matrix restricted crack coalescence and crack propagation in the interface and matrix region under cyclic loading. Consequently, nanoclay added CFRPCs held higher residual strength and stiffness compared to the control CFRPCs after similar number of fatigue cycles.
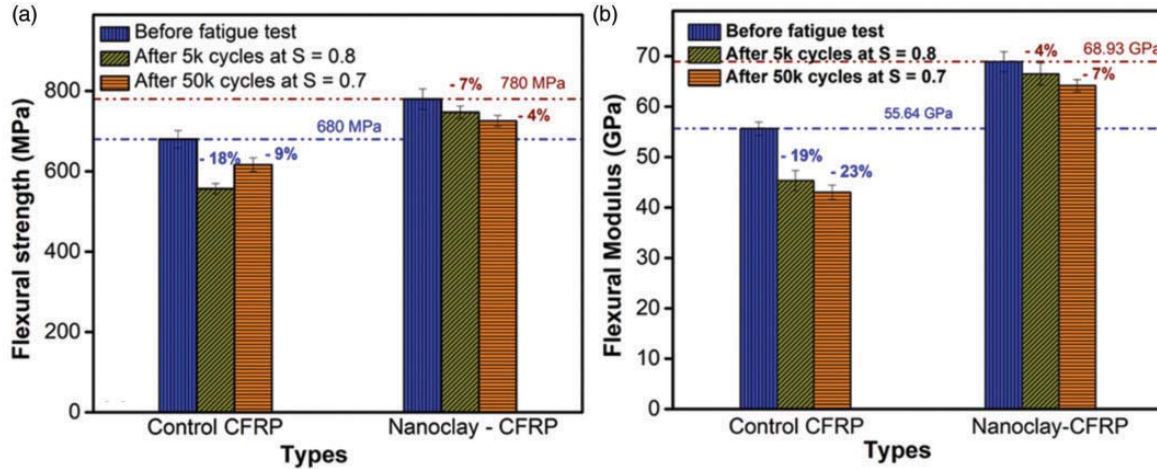
Figure 9. Comparison of the (a) residual fatigue strength and (b) modulus of control and nanoclay added CFRPCs after 5 K and 50 K cycles at 0.8 and 0.7 stress level, respectively.

Fracture toughness assessment

Load displacement behavior

The representative load vs. displacement $(P - \delta)$ plots for both control and nanoclay added CFRPCs are presented in Figure 10. Both types of the samples showed similar trend in $P - \delta$ curve that is characterized by the initial linear pattern representing elastic crack growth, followed by the non-linear rise in the curve indicating decrease in the stiffness. After the peak load point, the release of strain energy followed a sudden drop in load with corresponding stick-slip behavior in $P - \delta$ curve.[53] The stick-slip pattern in load-displacement curve is one of the distinct features of the woven fiber reinforced composite,[54] which can be attributed to the variation of fracture toughness through the crack propagation plane. This variation occurs due to the varying matrix thickness at the mid-plane and non-planar nature of woven carbon fabric that deflects the crack path, as the crack-front tries to follow the general contour of the fabric surfaces.[53] Another reason for the presence of stick-slip pattern in the load-displacement plot, is the fiber bridging which is depicted in Figure 10. The stick slip pattern is independent of the presence of nanoclay in the fracture surface, as stick-slip was observed for both types of the samples. Even though the stick slip behavior is independent of the addition of nanoclay, it is seen that nanoclay added CFRPCs exhibited higher load value in the $P - \delta$ plot throughout the whole fracture stages.

Critical interlaminar fracture characterization

The Mode I interlaminar fracture toughness was evaluated based on MBT following equation (3). The critical fracture toughness, G_{Ic} was evaluated in four different
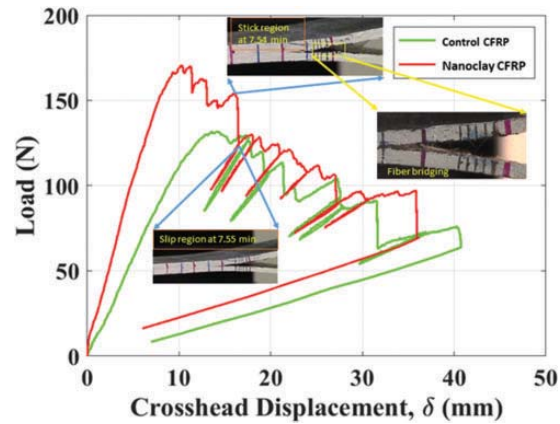

Figure 10. Representative load vs. displacement curves of control and nanoclay added CFRPCs in Mode I interlaminar fracture test.

ways of measuring the load/deflection as mentioned in ASTM standard.[42] These include: (i) VIS: the point at which delamination was visually observed at the edge of the specimen, (ii) NL: the global point of deviation from linearity in the load displacement plot, (iii) 5% COM: 5% increase in compliance point, and (iv) PEAK: peak load point in $P - \delta$ curve. It is evident form Figure 11(a) that the calculated G_{Ic}, followed the similar pattern as mentioned in the ASTM standard, where the G_{Ic} based on the VIS is in between the NL and 5% COM increment method.[42] From Figure 11(a), it is clearly seen that regardless of the data reduction techniques, nanoclay added samples showed significantly higher value of G_{Ic} compared to the control samples. The highest value of G_{Ic} was found to be 1670 J/m^2 for nanoclay added samples and 1260 J/m^2 for the control samples based on the
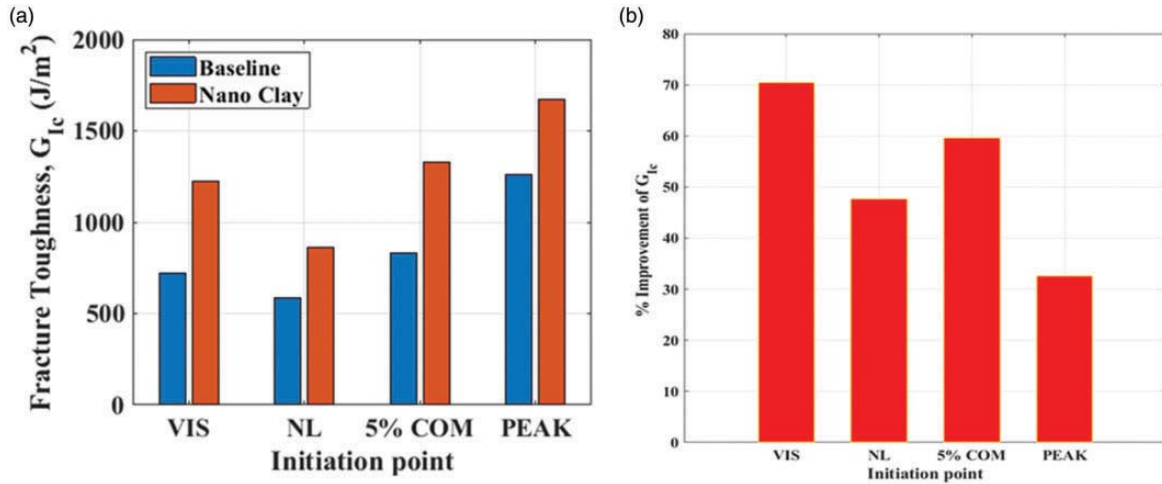
Figure 11. (a) Comparison of the critical fracture toughness (G_{Ic}) of control and nanocaly added CFRPCs, (b) %Improvement of fracture toughness due to the addition of Nanoclay at CFRPCs.
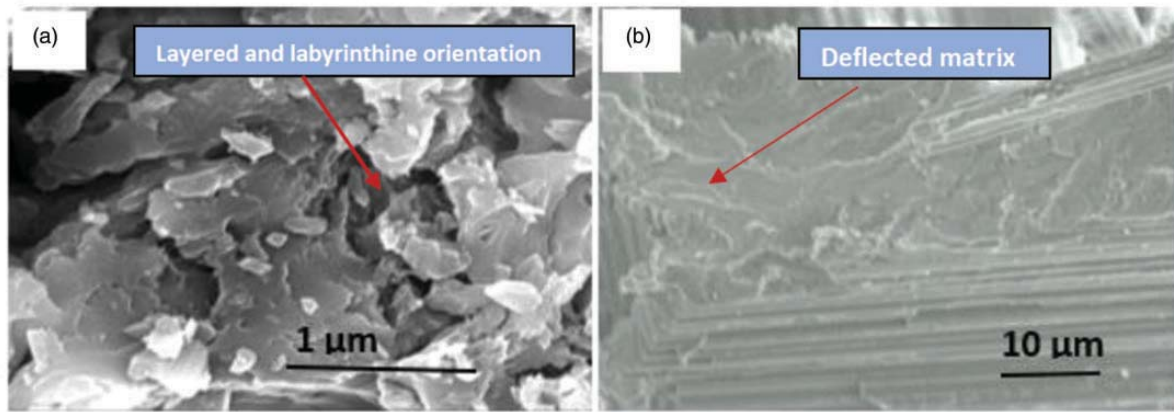

Figure 12. (a) Layered and labyrinthine orientation of nanoclay in the polymer matrix, (b) Fractured matrix showing the deflected area after fatigue test of nanoclay – CFRPC specimen.

peak load point calculation, which is an increase of over 32.5%. The improvement of the fracture toughness for each data reduction techniques is illustrated in Figure 11 (b), where the highest improvement was observed for the VIS method which was 70.5% compared to the reference specimen. This observation is consistent with the previous studies.[22]

Presence of layered-structure nanoclay in the polymer matrix create torturous and irregular orientation (Figure 12(a)) that bifurcate the propagating crack by reducing stress concentration at crack tip. As shown in Figure 12(b), fractured surface of nanoclay added matrix showed more irregular and deflected region after fracture test indicating that nanoclay added matrix absorbed higher energy by plastic deformation before fracture. Consequently, nanoclay added samples showed higher fracture toughness than the control samples.

Conclusion

The flexural fatigue test and detailed statistical analysis of fatigue life of the CFRPCs without and with nanoclay have been carried out. Fracture toughness of the composites also have been investigated and compared. Microstructural observation has been performed to indicate the change in microstructural and morphological features of the CFRPCs after adding nanoclay. The following are major outcomes of the study.

1. Addition of nanoclay in the epoxy matrix of the CFRPCs improved the static flexural strength and modulus by 15% and 24%, respectively.
2. More than 300% improvement in the mean and predicted fatigue life of CFRPCs has been achieved by incorporating nanoclay in the epoxy matrix.

3. The two-parameter Weibull function and sigmoidal model was found to reasonably characterize and predict the fatigue life of the CFRPCs without and with nanoclay.

4. Nanoclay added CFRPCs showed more than 2 times and 3 times higher residual fatigue strength and stiffness respectively then control CFRPCs throughout the whole fatigue life.

5. The value of critical fracture toughness, G_{Ic} was found to be 33–71% higher for the nanoclay added CFRPCs.

6. Incorporation of nanoclay improved stiffness of the polymer matrix. Nanoclay added matrix showed more plastic deformation that increased the overall fracture energy under cyclic loading. Fiber-matrix interfacial bonding was also significantly improved after addition of nanoclay. All these microstructural and morphological changes in the nanoclay added composites resulted in significantly improved fatigue and fracture performance.

This study can be an important contribution to the application of light composite materials associated with the cyclic loading. The work can be considered as a valuable resource and guideline for the design of composite materials as well as a motivation to carry similar analysis for other types of nanophased composites. However, more potential research can be conducted on the fatigue of nanoclay added CFRPCs considering the environmental effects, especially taking into considerations effects of temperature (both low and elevated), moisture and UV radiation, either in isolation or combined, to evaluate the benefits of known barrier properties of nanoclay.

Declaration of Conflicting Interests

The author(s) declared no potential conflicts of interest with respect to the research, authorship, and/or publication of this article.

ORCID iDs

Md Sarower Hossain Tareq https://orcid.org/0000-0001-8954-3295

Shaik Zainuddin https://orcid.org/0000-0002-7506-9358
Bodiuzzaman Jony https://orcid.org/0000-0001-6090-0228

References

1. Tehrani M, Boroujeni AY, Hartman TB, et al. Mechanical characterization and impact damage assessment of a woven carbon fiber reinforced carbon nanotube–epoxy composite. *Compos Sci Technol* 2013; 75: 42–48.

2. Kandare E, Khatibi AA, Yoo S, et al. Improving the through-thickness thermal and electrical conductivity of carbon fibre/epoxy laminates by exploiting synergy between graphene and silver nano-inclusions. *Compos Part Appl Sci Manuf* 2015; 69: 72–82.

3. Zhang W, Picu RC and Koratkar N. The effect of carbon nanotube dimensions and dispersion on the fatigue behavior of epoxy nanocomposites. *Nanotechnology* 2008; 19: 285709.

4. Zhang W, Picu RC and Koratkar N. Suppression of fatigue crack growth in carbon nanotube composites. *Appl Phys Lett* 2007; 91: 193109.

5. Saha S, Tareq SH and Galib RH. Effect of overageing conditions on microstructure and mechanical properties in Al–Si–Mg alloy. *J Mater Sci Eng* 2016; 5: 281.

6. Talreja R. Damage and fatigue in composites – a personal account. *Compos Sci Technol* 2008; 68: 2585–2591.

7. Stinchcomb WW and Reifsnider KL. Fatigue damage mechanisms in composite materials: a review. *Fatigue Mech* 1979; 675: 762-787.

8. Tareq MS, Zainuddin S, Woodside E, et al. Investigation of the flexural and thermomechanical properties of nanoclay/graphene reinforced carbon fiber epoxy composites. *J Mater Res* 2019; 34: 3678–3687.

9. Jamison RD, Schulte K, Reifsnider KL, et al. Characterization and analysis of damage mechanisms in tension-tension fatigue of graphite/epoxy laminates. *Eff Defects Compos Mater* 1984; 836: 21-55.

10. Reifsnider KL, Schulte K and Duke JC. Long-term fatigue behavior of composite materials. *Long-Term Behav Compos* 1983; 813: 136-159.

11. Khan SU, Munir A, Hussain R, et al. Fatigue damage behaviors of carbon fiber-reinforced epoxy composites containing nanoclay. *Compos Sci Technol* 2010; 70: 2077–2085.

12. Koloor SSR, Abdullah MA, Tamin MN, et al. Fatigue damage of cohesive interfaces in fiber-reinforced polymer composite laminates. *Compos Sci Technol* 2019; 183: 107779.

13. Song Q, Li K, Qi L, et al. The reinforcement and toughening of pyrocarbon-based carbon/carbon composite by controlling carbon nanotube growth position in carbon felt. *Mater Sci Eng A* 2013; 564: 71–75.

14. Boroujeni AY, Tehrani M, Nelson AJ, et al. Hybrid carbon nanotube–carbon fiber composites with improved in-plane mechanical properties. *Compos Part B Eng* 2014; 66: 475–483.

15. Jony B, Thapa M, Mulani S, et al. Repeatability of non-autonomous self-healing with thermoplastic healing agent in fiber reinforced thermoset composite. In: